

# Hyperfine Fields in an Ag/Fe Multilayer Film Investigated with $^8\text{Li}$ $\beta$ -Detected Nuclear Magnetic Resonance

T.A. Keeler,<sup>1</sup> Z. Salman,<sup>2,\*</sup> K.H. Chow,<sup>3</sup> B. Heinrich,<sup>4</sup> M.D. Hossian,<sup>1</sup> B. Kardasz,<sup>4</sup> R.F. Kiefl,<sup>1,2</sup> S.R. Kretziman,<sup>2</sup> C.D.P. Levy,<sup>2</sup> W.A. MacFarlane,<sup>5</sup> O. Mosendz,<sup>4</sup> T.J. Parolin,<sup>5</sup> M.R. Pearson,<sup>2</sup> and D. Wang<sup>1</sup>

<sup>1</sup>*Department of Physics and Astronomy, University of British Columbia, Vancouver, BC, Canada V6T 1Z1*

<sup>2</sup>*TRIUMF, 4004 Wesbrook Mall, Vancouver, Canada V6T 2A3*

<sup>3</sup>*Department of Physics, University of Alberta, Edmonton, AB, Canada T6G 2G7*

<sup>4</sup>*Department of Physics, Simon Fraser University, Vancouver, BC, Canada V5A 1S6*

<sup>5</sup>*Department of Chemistry, University of British Columbia, Vancouver, BC, Canada V6T 1Z1*

Low energy  $\beta$ -detected nuclear magnetic resonance ( $\beta$ -NMR) was used to investigate the spatial dependence of the hyperfine magnetic fields induced by Fe in the nonmagnetic Ag of an Au(40 Å)/Ag(200 Å)/Fe(140 Å) (001) magnetic multilayer (MML) grown on GaAs. The resonance line-shape in the Ag layer shows dramatic broadening compared to intrinsic Ag. This broadening is attributed to large induced magnetic fields in this layer by the magnetic Fe layer. We find that the induced hyperfine field in the Ag follows a power law decay away from the Ag/Fe interface with power  $-1.93(8)$ , and a field extrapolated to  $0.23(5)$  T at the interface.

The unique properties exhibited by thin layers of ferromagnetic metal separated by a layer of nonmagnetic metal spacer are both interesting and useful for applications in “spintronic” devices<sup>1</sup>. In these structures the coupling between the ferromagnetic layers oscillates between ferromagnetic (FM) and antiferromagnetic (AF) as a function of the thickness of the nonmagnetic spacer separating them<sup>2,3,4,5</sup>. This interlayer exchange coupling (IEC) is related to an oscillating electronic spin polarization induced in the nonmagnetic spacer due to the magnetic layers. The oscillation period ( $\sim 10$  Å)<sup>6</sup> is governed by the Fermi surface of the metal spacer. While several theoretical models have been developed to explain this behavior, it is difficult to establish which is the most “correct” since a direct measurement of the effects in the nonmagnetic spacer is challenging. These phenomena led to the discovery of the giant magneto-resistance (GMR) effect,<sup>7</sup> which is of great scientific interest, and also has important technological ramifications. For example, the drastic increase in hard disk bit density of the last 20 years was made possible by the vast increase in sensitivity of read heads that incorporate GMR structures. This sensitivity is a consequence of the strong field dependence of the resistivity of GMR structures.

The most well-known model developed to explain the FM-AF coupling oscillations in these systems is an extension of the Ruderman-Kittel-Kasuya-Yosida (RKKY) model describing the effect of a magnetic impurity on the conduction electrons of a nonmagnetic host metal<sup>8,9</sup>. The oscillations are the result of the sharp cutoff of wave-vectors at the Fermi surface in the spacer, resulting in an imperfect screening of the magnetic moments and oscillations in the polarization of conduction electrons. It is via this polarization that the magnetic layers are coupled. The period of oscillation is thus related to the Fermi surface, with period determined by the “critical spanning” wave-vectors of the spacer material<sup>10</sup>. In Ag there are two critical spanning vectors associated with the “neck” and “belly” regions of the Fermi surface in the (001) di-

rection.

The small amplitude of the induced electronic polarization (due to rapid decay away from the magnetic layer) as well as the small physical size of typical samples (spacer thicknesses typically several hundred Å or less) makes direct measurements of the induced polarization within the nonmagnetic spacer layer very difficult. To date, most quantitative methods used to measure the polarization in the spacer material are either averages of the polarization across the entire spacer, or probe the surface of a nonmagnetic overlayer grown on a ferromagnetic substrate. In particular it is very difficult/impossible to directly probe the spatial dependence of the conduction electrons polarization within the nonmagnetic layer. Such measurements require a technique that is sensitive to the local polarization of conduction electrons throughout the entire spacer. Mössbauer spectroscopy<sup>11</sup>, perturbed angular correlations<sup>12</sup>, and nuclear orientation<sup>13</sup> are local probes, but their limited sensitivity restricts them to measurements close the magnetic-nonmagnetic interface where the induced fields are strongest. In order to probe the behaviour deep within the non-magnetic layer one requires more sensitive measurements of the local polarization, such as low energy muons spin rotation (LE- $\mu$ SR)<sup>14,15</sup>. The technique used herein is depth resolved  $\beta$ -detected nuclear magnetic resonance ( $\beta$ -NMR).

In this paper we report the results of  $\beta$ -NMR measurements of the induced hyperfine field distribution in the nonmagnetic layer of a Ag(200 Å)/Fe(140 Å) magnetic multilayer (MML) prepared by molecular beam epitaxy (MBE) on a GaAs (001) single crystal substrate. We find that the induced hyperfine field in the Ag decays away from the Ag/Fe interface following a power law with exponent  $\alpha = -1.93(8)$ . One of the key parameters in theories describing this effect is the exponent  $\alpha$ , which is both difficult to measure or calculate. However, it has significant fundamental and practical importance since it determines how strongly two magnetic layers separated by a nonmagnetic spacer layer will couple.

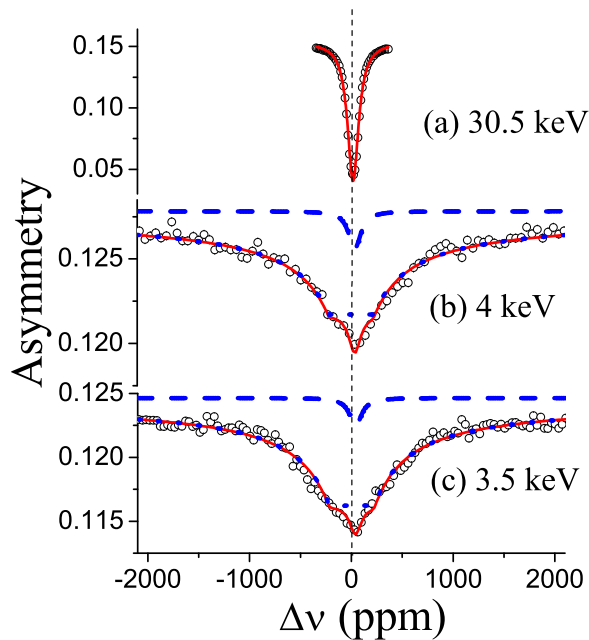


FIG. 1: (color online)  $\beta$ -NMR spectra measured in the MML sample at room temperature and a field of 4.5 T at implantation energy (a) 30.5 keV, (b) 4 keV and (c) 3.5 keV. The solid red lines are best fit to the calculated lineshapes (see text). The dotted/dashed lines represent the contribution from  $^8\text{Li}$  in Ag and Au respectively.

$\beta$ -NMR is a technique closely related to conventional nuclear magnetic resonance (NMR). However, in  $\beta$ -NMR the signal is generated using the  $\beta$ -decay properties of highly spin polarized radioactive nuclei ( $\sim 10^8$ ) that have been implanted directly into the sample, whereas conventional NMR relies on a much larger number ( $\sim 10^{18}$ ) of intrinsic nuclei to generate a signal.  $\beta$ -NMR experiments conducted in the ISAC facility at TRIUMF use a beam of spin polarized radioactive  $^8\text{Li}$  ( $I = 2, \gamma = 6301.5 \text{ kHz/T}$ ,  $\tau = 1.21 \text{ s}$ ) which is implanted into the sample and used as a spin probe. The  $^8\text{Li}$  nuclear polarization, which is the quantity of interest, is monitored through its beta decay where a high energy electron is emitted preferentially opposite to the direction of its nuclear spin. The polarization is measured as a function of the frequency of an applied transverse radio frequency (RF) field. The resulting resonance is a sensitive probe of the local internal electronic and magnetic environment. The implantation energy can be adjusted in the range 0.1–30.5 keV, corresponding to mean implantation depths of between 2 and 200 nm from the sample surface. Previous studies on an Au(40 Å)/Ag(800 Å)/Fe(14 Å) (001) film demonstrated our ability to make depth resolved  $\beta$ -NMR measurements in the different layers, as well as our sensitivity to the induced hyperfine fields in the Ag close to the Fe<sup>16</sup>. This ability to extract information about the local magnetic environment as a function of depth on a nm length scale

distinguishes low energy  $\beta$ -NMR from conventional  $\mu\text{SR}$  and NMR. It is similar to LE- $\mu\text{SR}$  in this respect but there are significant differences, e.g. the different time scale, so that the two methods are often complementary. A more complete description of the  $\beta$ -NMR technique can be found elsewhere<sup>17,18</sup>.

The Au(40 Å)/Ag(200 Å)/Fe(140 Å) MML sample was grown using MBE on a GaAs (001) single crystal substrate. The substrate was sputtered clean and annealed to yield large flat terraces on which a 140 Å Fe layer was grown. The small lattice mismatch between GaAs and Fe (-1.4 %) allows growth of body centered cubic (bcc) Fe (001) into well ordered layers. Then a 200 Å layer of face centered cubic (fcc) Ag was grown on Fe following the (001) orientation with its lattice rotated by  $\pi/4$ .<sup>19</sup> The sample was finally capped with a protective 40 Å Au layer. The thicknesses of the layers were monitored during growth using a calibrated quartz crystal microbalance.

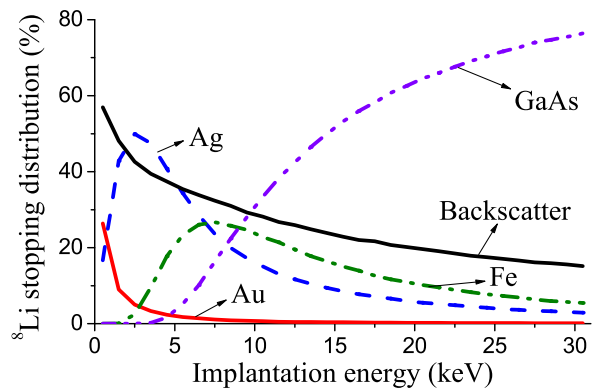


FIG. 2: (color online) Percentage of  $^8\text{Li}$  stopping in each layer of the MML sample as a function of implantation energy, calculated using TRIM.SP Monte-Carlo simulation.

The sample was placed in the  $\beta$ -NMR spectrometer in an applied magnetic field of 4.5 T normal to the film surface. Representative  $\beta$ -NMR spectra at room temperature and 3 different implantation energies are shown in Fig. 1. At full implantation energy (30.5 keV) most of the  $^8\text{Li}$  is implanted into the GaAs substrate. The resonance in Fig. 1(a) fits well to a Lorentzian lineshape with a width of 4 kHz, as expected for  $^8\text{Li}$  in GaAs.<sup>20</sup> Figs 1(b) and (c) show the spectra obtained with implantation energies 4.0 and 3.5 keV respectively. As shown in Fig. 2, at these energies TRIM.SP Monte-Carlo simulations<sup>21</sup> predict that most of the  $^8\text{Li}$  stops in the Ag layer ( $\sim 50\%$ ), with a small amount ( $\sim 3\%$ ) stopping in the Au layer. The remaining  $^8\text{Li}$  is backscattered ( $\sim 37\%$ ) or stops in the Fe ( $\sim 10\%$ ). Note, since backscattered  $^8\text{Li}$  stops outside the RF coil they do not contribute to the measured resonance line. Similarly,  $^8\text{Li}$  stopping in Fe experiences a very large magnetic field and therefore produces

a resonance outside our frequency window<sup>22</sup>. Recent  $\beta$ -NMR measurements show that the intrinsic  $^8\text{Li}$  resonance linewidth in a thin Ag film is  $0.5 - 1$  kHz.<sup>18</sup> In contrast, the linewidth observed in Fig. 1(b) and (c) is an order of magnitude larger. This broadening is attributed to the induced hyperfine magnetic field in Ag due to the Fe magnetic layer.

We now discuss the modelling of the lineshapes obtained, such as those shown in Fig. 1. Following the RKKY-based theoretical description<sup>23</sup>, the induced hyperfine field in Ag as a function of the distance ( $x$ ) from an ideal Ag/Fe interface, follows

$$B(x) = \sum_{i=0}^1 B_i \left( \frac{x}{\lambda_i} \right)^{\alpha_i} \sin \left( \frac{2\pi x}{\lambda_i} + \phi_i \right), \quad (1)$$

where  $\lambda_i = 2\pi/k_i$  are the Fermi wavelengths associated with the two critical spanning vectors, i.e. the belly and neck. The expected resonance lineshape, representing the magnetic field probability distribution for the implanted  $^8\text{Li}$ , is calculated using Eq. (1), and the stopping  $^8\text{Li}$  profile in the Ag layer determined using TRIM.SP calculations (Fig. 3). An example calculated using Eq. (1),

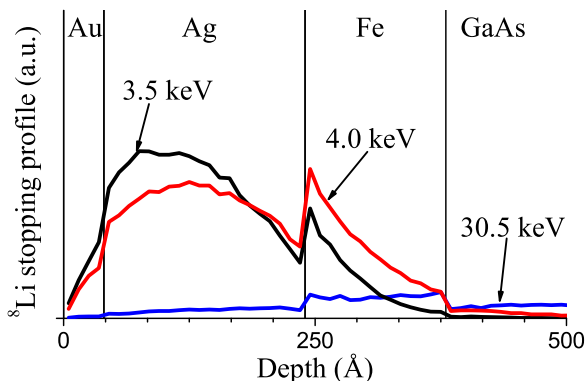


FIG. 3: (color online) The  $^8\text{Li}$  stopping profile in the MML sample generated using TRIM.SP Monte-Carlo simulations for implantation energies of 3.5, 4.0 and 30.5 keV. At lower energies  $^8\text{Li}$  stops predominantly in the Ag layer, while at the full energy nearly all  $^8\text{Li}$  stops in the GaAs substrate.

with a contribution only from the belly spanning vector ( $\lambda = 11.7$  Å,  $\alpha = -1.9$ ,  $B_0 = 0.23$  T and  $B_{ext} = 4.5$  T.), is shown in Fig 4(a). The contribution from the neck spanning vector is negligible, since its associated wave length ( $\sim 4.85$  Å) is on the same length scale of the distance between neighboring implanted  $^8\text{Li}$ , and hence its contribution is averaged out over the  $^8\text{Li}$  stopping sites in the Ag lattice. The distinguishing features of this lineshape are the peaks on either side of the applied field ( $B_{ext}$ ) resulting from Van Hove singularities. The large inner double peaks result from the non-zero hyperfine fields at the Ag farthest from the Ag/Fe interface. However, it has been shown that even slight interface

roughness tends to wipe out the short wavelength oscillations in the electron polarization<sup>24</sup> since the distance to the interface no longer has a well defined value over lateral distances larger than the terrace width. Furthermore a vertical mismatch between atomic planes, as little as 0.8% for Ag/Fe(001) also leads to suppression of both the long and short wavelengths.<sup>25</sup> The  $^8\text{Li}$  beam averages over the area of the beam spot ( $\sim 3$  mm diameter), therefore we do not expect to observe oscillations of the induced hyperfine fields. This will have the effect of “smearing” out the oscillations in the induced field [Eq. (1)]. Therefore we use a phenomenological form for the induced field distribution:

$$B_{max}(x) = \frac{B_0}{1 + (\lambda_F/x)^\alpha} \quad (2)$$

with  $\lambda_F = 2\pi/k_F$  taken as the long period Fermi wavelength of Ag (11.7 Å). We assume that at a particular distance,  $x$ , from the interface, the hyperfine field is equally likely<sup>26</sup> to have any value between  $B_{ext} \pm B_{max}$ . This form has several advantages: 1) it gives a value of  $B_0$  for the hyperfine field right at the Ag/Fe interface, 2) it maintains the asymptotic power law behaviour,  $x^\alpha$ , predicted by RKKY, 3) it avoids the unphysical divergent behaviour at the Ag/Fe interface in Eq. (1). The lineshape, shown in Fig 4(b), results from this form of field distribution. Note that it does not have the peaks associated with the oscillating magnetic field, but it is symmetric and exhibits a characteristic “flat top”. This low field cutoff originates from the fact that the hyperfine field does not decay to zero at the Ag/Au interface. This lineshape is consistent with the  $\beta$ -NMR spectra in Figs 1(a) and (b).

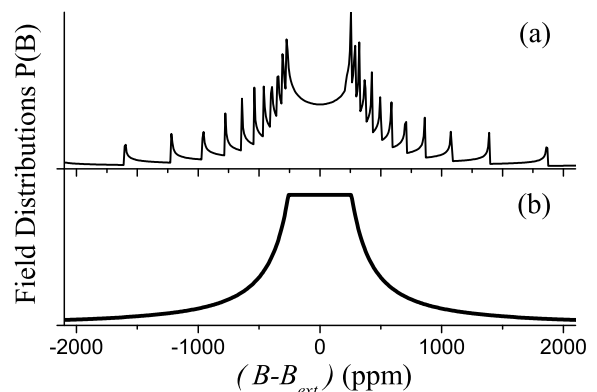


FIG. 4: Simulated lineshape, in an applied field  $B_{ext}$ , generated for induced hyperfine fields that follows (a) an oscillating distribution described by Eq. (1) and (b) a uniform distribution within the envelope described by Eq(2). Both lineshapes were calculated using  $\lambda = 11.7$  Å,  $\alpha = -1.9$ ,  $B_0 = 0.23$  T and  $B_{ext} = 4.5$  T.

Note that, in contrast to the calculation above and the

lineshape in Fig. 4(b), the experimental  $\beta$ -NMR spectra show a sharp peak and not a “flat top” feature. This is attributed to the small amount of  $^8\text{Li}$  that stops in the thin Au capping layer (dashed lines in Fig. 4(b) and (c)). These spectra were fit to the sum of our model lineshape, Fig 4(b), and a Lorentzian to account for the small signal from Au. The contribution to the measured resonances from Ag and Au, as obtained from the fit, are represented by the dotted and dashed lines in Fig. 1 respectively. The induced field parameters extracted from the fits in Fig. 1(b) and (c) are  $\alpha = -1.93(8)$  and  $B_0 = 0.23(5)$  T (common for both spectra). The Lorentzian fit for the resonance in Au was found to be  $\sim 4$  kHz wide, and shifted approximately +40 parts per million (ppm) relative to the GaAs reference. The Knight shift of the Au is comparable with previous measurements of intrinsic Au (+60(20) ppm)<sup>27</sup>, but the width is about twice that of previous measurements. This may be due to the higher RF power used in these experiments but could also be due to the induced fields from Fe extending into the Au layer. In addition, we find that the ratio of the contribution from Au to Ag from the fit parameters (i.e. the ratio of the areas of the resonance in Au to that in Ag) is  $\sim 3\%$ , in reasonable agreement with  $\sim 6\%$  from TRIM.SP calculations (Fig. 2). The 3% difference may be due to the limited accuracy of TRIM.SP in predicting ion implantation profiles especially at low implantation energies.<sup>21,28</sup>

The extracted value of  $B_0 = 0.23(5)$  T, which is the hyperfine coupling of  $^8\text{Li}$  at the Ag/Fe interface, is in reasonable agreement with the calculated value 0.30 T for the induced hyperfine field at the first Ag layer at the interface.<sup>29</sup> Also the asymptotic power of the induced field,  $\alpha = -1.93(8)$ , agrees very well with the theoretical value  $-2$  predicted by RKKY theory.<sup>23,24,30</sup> It is however larger than the values  $\alpha = -0.4(1)$  and  $-0.8(1)$  measured using LE- $\mu$ SR in Fe(40 Å)/Ag(3000 Å)(001)<sup>14</sup> and Fe(40 Å)/Ag(200 Å)/Fe(40 Å)(001)<sup>15</sup> samples, respectively. Similarly, using Cu NMR to measure the spin polarization profile in multilayers of Ni/Cu, Goto *et al.*<sup>31</sup> found  $\alpha = -1$ . In all those measurements, induced fields of the form Eq.(1) were assumed and the magnetic field parallel to the surface was used to perform these measurements, while in our measurements the field was applied perpendicular to the surface. In principle, this should

not affect the value of  $\alpha$ <sup>31</sup>. The source of discrepancy between our results and those from Refs.<sup>14,15,31</sup> may be the reduced sensitivity of the previous measurements to the interface region. In the LE- $\mu$ SR measurements, the contribution of the 3 nm region of the Ag/Fe interface is negligible<sup>14</sup>, since the muons in this region experience a field which is too high to be measured. Note that both NMR and LE- $\mu$ SR measurements are performed in the time domain, i.e. the high field contribution occurs at early times, therefore the dead time associated with the measurement decreases the sensitivity to high field regions (interface). In contrast our measurements are performed directly in the frequency domain and therefore have no such effect (provided that one sweeps a sufficiently large frequency range). In addition, in NMR measurements it is extremely hard to account for the contribution of all nuclei in the spacer since the resonance cannot be normalized, while the method of detection used in  $\beta$ -NMR enables detection of the signal from all implanted spin probe nuclei. Finally, we would like to point out that calculation based on the quantum-interference model<sup>32</sup> predict an oscillating polarization that involved three terms with  $\alpha = -1, -2$  and  $-3$ . Thus, it may be that the different techniques are sensitive to different terms.

In conclusion, we have carried out depth resolved low energy  $^8\text{Li}$   $\beta$ -NMR to measure directly the hyperfine field profile in an Ag layer induced by a magnetic Fe layer. No indication of an oscillating hyperfine field is observed. However, we find that the induced fields decrease away from the Ag/Fe interface following an asymptotic power law  $x^{-1.93(8)}$  in good agreement with theoretical calculations based on RKKY theory. The induced field at the Ag/Fe interface  $B_0 = 0.23(5)$  T is also in good agreement with calculations.

This research was supported by the Center for Materials and Molecular Research at TRIUMF, the Natural Sciences and Engineering Research Council of Canada and the Canadian Institute for Advanced Research. We would like to thank W. Eckstein from MPI fur Plasmaphysik in Garching, Germany, who developed the TRIM.SP code we used to generate the stopping profiles. We would especially like to thank Rahim Abasalti, Basam Hitti, and Donald Arseneau for their expert technical support.

\* Email address: z.salman1@physics.ox.ac.uk; Current address: Clarendon Laboratory, Department of Physics, Oxford University, Parks Road, Oxford OX1 3PU, UK

<sup>1</sup> B. Heinrich and J.F. Cochran, *Adv. Phys.* **42**, 523 (1993).

<sup>2</sup> P. Grunberg, R. Schreiber, Y. Pang, M. B. Brodsky and H. Sowers, *Phys. Rev. Lett.* **57**, 2442 (1986).

<sup>3</sup> B. Heinrich, Z. Celinski, J. F. Cochran, W. B. Muir, J. Rudd, Q. M. Zhong, A. S. Arrott, and K. Myrtle, and J. Kirschner, *Phys. Rev. Lett.* **64**, 673 (1990).

<sup>4</sup> S.S.P. Parkin, N. More, and K. P. Roche, *Phys. Rev. Lett.*

**64** 2304 (1990).

<sup>5</sup> S. S. P. Parkin and D. Mauri, *Phys. Rev. B* **44**, 7131 (1991)

<sup>6</sup> S.S.P. Parkin, *Phys. Rev. Lett.* **67**, 3598 (1991).

<sup>7</sup> IEC is generally not a necessary condition for observing the GMR effect. However, if one does not have a spin-valve structure, an antiferromagnetic coupling is necessary to observe the GMR effect.

<sup>8</sup> D. M. Edwards, J. Mathon, R. B. Muniz, and M. S. Phan, *Phys. Rev. Lett.* **67**, 493-496 (1991).

<sup>9</sup> P. Bruno and C. Chappert, *Phys. Rev. B* **46**, 261 (1992).

- <sup>10</sup> M.D. Stiles, *Journ. Mag. Mater.* **200**, 322 (1999).
- <sup>11</sup> Y. Kobayashi, S. Nasu, T. Emoto, and T. Shino, *Hyperfine Interact.* **111**, 129 (1998).
- <sup>12</sup> B.-U. Runge et al., *Phys. Rev. Lett.* **79**, 3054 (1997).
- <sup>13</sup> T.Phalet, M.J. Prandolini, W.D. Brewer, P. Schuurmans, N. Severijns, B.G. Turrell, B. Vereecke, and S. Versyck, *Phys. Rev. B* **71**, 144431 (2005).
- <sup>14</sup> H. Luetkens, J. Korecki, E. Morenzoni, T. Prokscha, A. Suter, M. Birke, N. Garifanov, R. Khasanov, T. Slezak and F.J. Litterst, *J. Magn. Mater.* **272-276**, 1128 (2004).
- <sup>15</sup> H. Luetkens, J. Korecki, E. Morenzoni, T. Prokscha, M. Birke, H. Gluckler, R. Khasanov, H.-H. Klauss, T. Slezak, A. Suter, E.M. Forgan, Ch. Niedermayer, and F.J. Litterst, *Phys. Rev. Lett.* **91**, 017204 (2003).
- <sup>16</sup> T. A. Keeler, Z. Salman, K. H. Chow, B. Heinrich, M. D. Hossain, B. Kardasz, R. F. Kiefl, S. R. Kreitzman, W. A. MacFarlane, and O. Mosendz, *Physica B* **374-375C**, 79 (2006).
- <sup>17</sup> R.F. Kiefl *et al.*, *Physica B* **326**, 189 (2003); Z. Salman, E.P. Reynard, W.A. MacFarlane, K.H. Chow, J. Chakhalian, S.R. Kreitzman, S. Daviel, C.D.P. Levy, R. Poutissou, and R.F. Kiefl, *Phys. Rev. B* **70**, 104404 (2004); Z. Salman, R.F. Kiefl, K.H. Chow, M.D. Hossain, T.A. Keeler, S.R. Kreitzman, C.D.P. Levy, R.I. Miller, T.J. Parolin, M.R. Pearson, H. Saadaoui, J.D. Schultz, M. Smadella, D. Wang, and W.A. MacFarlane, *Phys. Rev. Lett.* **96**, 147601 (2006); T.J. Parolin, Z. Salman, J. Chakhalian, Q. Song, K.H. Chow, M.D. Hossain, T.A. Keeler, R.F. Kiefl, S.R. Kreitzman, C.D.P. Levy, R.I. Miller, G.D. Morris, M.R. Pearson, H. Saadaoui, D. Wang, and W.A. MacFarlane, *Phys. Rev. Lett.* **98**, 047601 (2007); Z. Salman, A.I. Mansour, K.H. Chow, M. Beaudoin, I. Fan, J. Jung, T.A. Keeler, R.F. Kiefl, C.D.P. Levy, R.C. Ma, G.D. Morris, T.J. Parolin, D. Wang, and W.A. MacFarlane, *Phys. Rev. B* **75**, 073405 (2007); Z. Salman, D. Wang, K.H. Chow, M.D. Hossain, S. Kreitzman, T.A. Keeler, C.D.P. Levy, W.A. MacFarlane, R.I. Miller, G.D. Morris, T.J. Parolin, H. Saadaoui, M. Smadella, and R.F. Kiefl, *Phys. Rev. Lett.* **98**, 167001 (2007); Z. Salman, K.H. Chow, R.I. Miller, A. Morello, T.J. Parolin, M.D. Hossain, T.A. Keeler, C.D.P. Levy, W.A. MacFarlane, G.D. Morris, H. Saadaoui, D. Wang, R. Sessoli, G.G. Condorelli, and R.F. Kiefl, *Nano Lett.* **7**, 1551 (2007).
- <sup>18</sup> G.D. Morris, W.A. MacFarlane, K.H. Chow, Z. Salman, D.J. Arseneau, S. Daviel, A. Hatakeyama, S.R. Kreitzman, C.D.P. Levy, R. Poutissou, R.H. Heffner, J.E. Elenewski, L.H. Greene, and R.F. Kiefl, *Phys. Rev. Lett.* **93**, 157601 (2004);
- <sup>19</sup> P. Etienne, J. Massies, F. Nguyen-Van-Dau, A. Barthelemy, and A. Fert, *Appl. Phys. Lett.* **55** (21), (1989), 2239.
- <sup>20</sup> K. H. Chow, Z. Salman, W.A. MacFarlane, B. Campbell, T.A. Keeler, R.F. Kiefl, C.D.P. Levy, G.D. Morris, T.J. Parolin, R. Poutissou and Z. Yamani, *Physica B* **374-375C**, 415 (2006).
- <sup>21</sup> W. Eckstein, *Computer Simulation of Ion-Solid Interactions* (Springer, Berlin, 1991).
- <sup>22</sup> K. Matsuta, M. Sasaki, T. Tsubota, S. Kaminaka, S. Kudo, M. Ogura, K. Arimura, M. Mihara, M. Fukuda, H. Akai, and T. Minamisono, *Hyperfine Interact.* **136**, 379 (2001).
- <sup>23</sup> P. Bruno and C. Chappert, *Phys. Rev. Lett.* **67**, 1602 (1991).
- <sup>24</sup> Y. Wang, P.M. Levy, and J.L. Fry, *Phys. Rev. Lett.* **65**, 2732 (1990).
- <sup>25</sup> Z. Celinski, B. Heinrich, *J. Magn. Mater.* **99**, L25 (1991); B. Heinrich, Z. Celinski, J.F. Cochran, A.S. Arrott, K. Myrtle, and S.T. Purcell, *Phys. Rev. B* **47**, 5077 (1993).
- <sup>26</sup> Models where increased weight is given to the extrema regions ( $B_{ext} \pm B_{max}$ ) were also considered. However, the fitting parameters and lineshapes produced were very similar to those obtained using the simpler model. Therefore we used the simpler model to analyse our results.
- <sup>27</sup> W.A. MacFarlane, G.D. Morris, T.R. Beals, K.H. Chow and R.A. Baartman, S. Daviel, S.R. Dunsiger, A. Hatakeyama and S.R. Kreitzman, C.D.P. Levy R.I. Miller, K.M. Nichol and R. Poutissou and R.F. Kiefl, *Physica B* **326**, 213 (2003).
- <sup>28</sup> E. Morenzoni, H. Glucker, T. Prokscha, R. Khasanov, H. Luetkens, M. Birke, E. M. Forgan, C. Niedermayer, M. Pleines, *Nuc. Inst. Meth. Phys.* **192**, 254 (2002).
- <sup>29</sup> C.O. Rodriguez, M.V. Gandulgia-Pirovana, E.L. Peltzer y Blancá, M. Petersen, and P. Novák, *Phys. Rev. B* **63**, 184413 (2001).
- <sup>30</sup> Y. Yafet, *Phys. Rev. B* **36**, 3948 (1987).
- <sup>31</sup> A. Goto, H. Yasuoka, H. Yamamoto and T. Shinjo, *J. Phys. Soc. Jap.* **62**, 2129 (1993).
- <sup>32</sup> K. Ishiji, H. Hashizume, Y. Suzuki and E. Tamura, *Phys. Rev. B* **74**, 174432 (2006).